Applied Energy 99 (2012) 414–422

Contents lists available at SciVerse ScienceDirect

Applied Energy

journal homepage: www.elsevier.com/locate/apenergy

A direct control based maximum power point tracking method for photovoltaic system under partial shading conditions using particle swarm optimization algorithm

Kashif Ishaque [a,b], Zainal Salam [a,*], Amir Shamsudin [a], Muhammad Amjad [a]

[a] Faculty of Electrical Engineering, Universiti Teknologi Malaysia, UTM 81310 Skudai, Johor Bahru, Malaysia
[b] Karachi Institute of Economics and Technology, Karachi 75190, Pakistan

HIGHLIGHTS

- A direct control MPPT approach for PV system using particle swarm optimization algorithm.
- Proposed method does not require PI control loops which normally exist in the PV system.
- It successfully tracks the global maxima of PV array under partial shading conditions.
- Proposed method yields an average MPPT efficiency of 99.5% for a whole day profile.

GRAPHICAL ABSTRACT

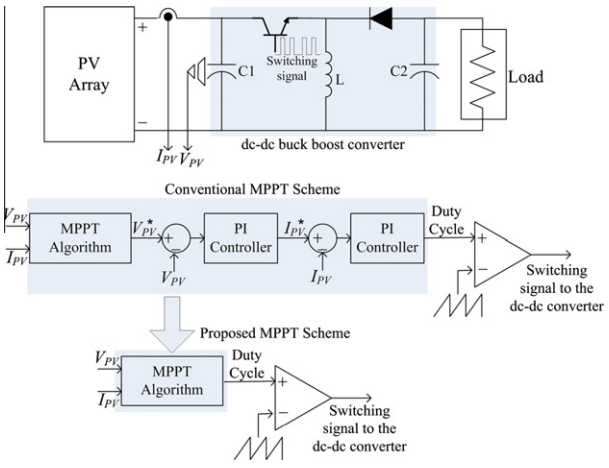

ARTICLE INFO

Article history:
Received 27 August 2011
Received in revised form 8 May 2012
Accepted 24 May 2012
Available online 30 June 2012

Keywords:
Partial shading
Direct control
Particle swarm optimization (PSO)
Maximum power point tracking (MPPT)
Photovoltaic (PV) system
Malaysian weather condition

ABSTRACT

This paper presents maximum power point tracking (MPPT) of photovoltaic (PV) system using particle swarm optimization (PSO) algorithm. The key advantage of the proposed technique is the elimination of PI control loops using direct duty cycle control method. Furthermore, since the PSO is based on optimized search method, it overcomes the common drawback of the conventional MPPT, i.e. the inability to track the global maximum point (GP) of PV array under partial shading conditions. The algorithm is employed on a buck-boost converter and tested experimentally using a PV array simulator. Ten irradiance patterns are imposed on the array, the majority of which include various partial shading patterns. Compared to the conventional direct duty cycle method, the proposed method performs excellently under all shading conditions. Finally, the performance of the proposed method is tested using the measured data of a tropical country (Malaysia) from 8.00 am to 6.00 pm. For the 10 h (daytime) irradiance and temperature profile, it yields an average MPPT efficiency of 99.5%.

1. Introduction

Solar energy is envisaged to be an important source of energy in the future. In particular, the solar photovoltaic (PV) power system

* Corresponding author. Tel.: +60 75536187; fax: +60 75566272.
E-mail addresses: kashif@fkegraduate.utm.my (K. Ishaque), zainals@fke.utm.my (Z. Salam).

0306-2619/$ - see front matter © 2012 Elsevier Ltd. All rights reserved.
http://dx.doi.org/10.1016/j.apenergy.2012.05.026

is becoming a popular renewable energy source due to its environmental friendliness with long term economic prospect. However, due to the high initial cost of PV system, the available solar energy needs to be the optimally captured. Enormous amount of work has been carried out to enhance the solar cell design and its fabrication technologies [1–8]. Whilst these efforts are crucial, it is equally important to continually improve the overall performance at the system level. One area of immense interest is the maximum power point tracker (MPPT). The aim of MPPT is to ensure that at any environmental condition (irradiance and temperature), the maximum power is extracted from the PV modules by matching its *P–V* operating point with the corresponding power converter.

Due to the non-linear characteristics *I–V* of the PV curve, the tracking of the maximum power point (MPP) at various environmental conditions can sometimes be a challenging task. The issue becomes more complicated when the entire PV array does not receive uniform irradiance – a condition known as partial shading (PS) [9]. When a PV array is subjected to PS, its *P–V* curves exhibit multiple peaks with several local and one global peak (GP), i.e. the problem is transformed from single to multi modal. The drawback with the conventional MPPT is that for majority of the cases, the algorithm is likely to trap at the local peak simply because it could not differentiate the local with the GP. Consequently, it oscillates around the vicinity of the local peak and will remain in that location indefinitely. As a result output power is reduced [10].

To date, numerous conventional MPPT schemes have been proposed; among the more popular ones are the hill climbing [11], perturb and observe (P&O) [12], incremental conductance [13,14], ripple correlation [15], short circuit current [16] and open-circuit voltage approaches [17]. Many of these, particularly the first three, are practically implemented in existing PV systems. Hill climbing (HC) is based on the perturbation in the duty cycle of the connected power converter. It is also known as the direct duty cycle method. The P&O, although similar in concept to HC, perturbs the operating voltage/current of the PV array. It works satisfactorily when the irradiance varies very slowly but is ineffective when subjected to sudden change in environmental condition. Incremental conductance works by incrementally comparing the ratio of derivative of conductance with the instantaneous conductance. More recently, various researcher employed artificial intelligence methods that include Fuzzy [18] and Neural Network [19]. These methods are very effective in dealing with the nonlinear characteristics of the *I–V* curves. However, they require extensive computational effort; for example, FL has to deal with fuzzification, rule base storage, inference mechanism and defuzzification operations. For ANN, large amount of data for training could be a major source of constraint. The matter becomes more crucial due to the dynamic nature of the PV systems; i.e. has to adopt changes in real time.

All the aforementioned methods, while operate satisfactorily under uniform irradiance, often fail to perform in PS. To overcome this drawback, numerous modifications to the conventional algorithms have been proposed [20–24]. In [20], a two-stage approach to track the GP was developed. Initially, the algorithm operates in the vicinity of the GP; then, this information is used to track GP in the second stage. Although effective, the method cannot track the GP for all environmental conditions. In [21], a compensation method for PV power is proposed; when the shading occurs, it activates the corresponding bypass diodes of the PV module according to the shaded level. However, this method only works well when PV array is in the series parallel (SP) configuration. In [22], a search algorithm with improved Fibonacci search is proposed. However, this method too cannot guarantee the tracking of GP under all shading conditions. Authors in [23], proposes another work two mode MPPT to track the GP. Global mode is activated due to the sudden change in operating power and MPPT begins to track all the possible local MPPs; this helps to distinguish the GP among all local peaks. Consequently, the system satisfactorily operates at the GP in the local mode. The drawback is that in certain shading conditions, it needs to scan almost 80% of the *I–V* curve to locate the GP, eventually affecting the dynamic performance of the PV system. In [24], a dividing rectangle (DIRECT) search method in conjunction with the P&O is proposed. The occurrence of PS condition activates the DIRECT algorithm, which locates the GP; once the GP is determined, the algorithm switches to P&O to maintain the tracking job. Despite the effectiveness of the algorithm, it is relatively complex and requires substantial computing effort.

Furthermore, most MPPT systems require two independent control loops to track the MPP. The first loop produces the reference signal in conjunction with the MPPT algorithm while the second is usually a (proportional) P or (proportional plus integral) PI controller. The latter is used to maintain the zero error at MPP [14]. The various advantages of PI make it very popular in wide variety of linear controllers. However, in nonlinear application such as the PV, these controllers do not work efficiently [25]. Furthermore, the unpredictable environmental variation does not suit the PI very well. Therefore, it is desirable to remove the PI from the control loop.

Recently, Evolutionary Algorithms (EAs) techniques have gained much attention due to its ability to handle multi-modal objective functions [26,27]. Since the *I–V* curves exhibits multi modal characteristics during PS, the EA methods seem to be well suited to track the GP under this condition. Among the EA techniques, the particle swarm optimization (PSO) method has a simple structure that can be effectively used for MPP tracking. Hence several authors have attempted to apply it; for example, in [28], PSO is applied in the constant bus voltage application. Despite its effectiveness, the algorithm developed by the authors cannot guarantee the tracking of GP for all shading conditions. In another work [29], an Adaptive Perceptive Particle Swarm Optimization (APPSO) is proposed for the same constant bus voltage application. However, due to additional dimensional search space, the number of particles needs to be increased compared to its original counterpart [28]. The increased number of particles eventually increases the computation burden, thus making real-time implementation more difficult. Besides, in the PSO exploration stage, more particles increase fluctuations in the operating power of PV array.

In this paper, PSO strategy with direct control is proposed. Both PI control loops are eliminated and duty cycle is adjusted directly in the algorithm. The objective is to improve the GP tracking in all conditions including the PS. The proposed work will demonstrate that sophisticated MPPT methods are not necessarily required and the desirable results can be achieved by employing a simple controller. Practically, the proposed system is investigated with a dc-dc buck-boost converter configured as MPPT. The PSO algorithm is implemented using a Dspace DS1104 [30] Digital Signal Processor (DSP) which is explicitly configured to optimize the control actions.

The remainder of the paper is organized as follows: the next section discusses about the characteristics of PV array subjected to PS. Section 3 presents an overview of PSO algorithm. This is followed by the MPPT structure of the proposed work. The application of PSO algorithm is given in Section 5. While in Section 6, the experimental setup of the proposed method is shown. Tracking results are discussed in the next section which also includes the real testing performance analyses of Malaysian weather for 10 h (from 8.00 am to 6.00 pm). Finally, the conclusions are made in the last section.

2. PV system under partially shaded (PS) condition

2.1. Modeling of PV array

In PV power generation, a centralized inverter topology is commonly utilized due to economic reasons. A single (centralized)

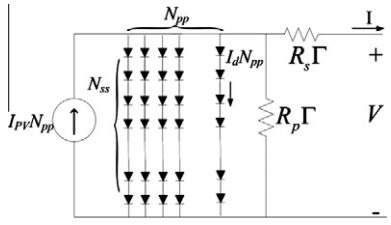

Fig. 1. Series parallel combination of PV array.

inverter is connected to a large number of PV modules, typically, in a series-parallel (SP) configuration. Fig. 1 shows a generalized SP configuration of a PV array. In this figure, one diode represents a PV module. For each module, the output current of the module can be described as [31]:

$$I = I_{PV} - I_{01}\left[\exp\left(\frac{V+IR_S}{a_1V_{T1}}\right)-1\right] - I_{02}\left[\exp\left(\frac{V+IR_s}{a_2V_{T2}}\right)-1\right] - \left(\frac{V+IR_s}{R_p}\right) \quad (1)$$

where I_{PV} is the current generated by the incidence of light. I_{o1} and I_{o2} are the reverse saturation currents of diode 1 and diode 2, respectively. The I_{o2} term is introduced to compensate for the recombination loss in the depletion region as described in [31]. Other variables are defined as follows: $V_{T\,1,2}$ ($=N_s\,kT/q$) is the thermal voltage of the PV module having N_s cells connected in series, q is the electron charge (1.60217646×10^{-19} C), k is the Boltzmann constant (1.3806503×10^{-23} J/K) and T is the temperature of the p–n junction in K. Variables a_1 and a_2 represent the diode ideality constants. Although greater accuracy can be achieved using this model (compared to the single diode model), it requires the computation of seven parameters, namely I_{PV}, I_{o1}, I_{o2}, R_p, R_s, a_1 and a_2. To simplify, several researchers assumed $a_1 = 1$ and $a_2 = 2$. The values are chosen based on the approximations of the Schokley-Read-Hall recombination in the space charge layer in the photodiode [31].

Recently, a simplified two diode model is proposed in [32]. The main advantage of this model is the simplification of the current equation, in which only four parameters are required, compared to six or more in the previously developed two-diode models as given in Eq. (1). The output equation of this model is given as:

$$I = I_{PV} - I_o\left[\exp\left(\frac{V+IR_s}{V_T}\right)+\exp\left(\frac{V+IR_s}{(p-1)V_T}\right)-2\right] - \left(\frac{V+IR_s}{R_p}\right) \quad (2)$$

$$I_{PV} = (I_{SC\_STC} + K_i\Delta T)\frac{G}{G_{STC}} \quad (3)$$

where I_{SC_STC} (in Ampere) is the light generated current at standard testing condition (STC), $\Delta T = T - T_{STC}$ (in Kelvin, $T_{STC} = 25$ °C), G is the surface irradiance of the cell and G_{STC} (1000 W/m^2) is the irradiance at STC. The constant K_i is the short circuit current coefficient, normally provided by the manufacturer. In [32], a new analytical equation of both saturation currents is derived. Both saturation currents can be calculated as:

$$I_{o1} = I_{o2} = I_o = \frac{(I_{SC\_STC} + K_i\Delta T)}{\exp[(V_{OC,STC} + K_v\Delta T)/\{(1+a_2)/p\}V_T] - 1} \quad (4)$$

$$p = 1 + a_2 \geqslant 2.2 \quad (5)$$

where $V_{OC,STC}$ (in voltages) is the open circuit voltage at STC. The constant K_v is the temperature coefficient of $V_{OC,STC}$; this value is available from the datasheet. The remaining two parameters R_s and R_p in Eq. (1) are calculated using iteration technique [32]. The equalization simplifies the computation as no iteration is required; the solution can be obtained analytically.

Using this simplified model, the output equation for the entire array in Fig. 1 can be written as:

$$I = N_{pp}\left\{I_{PV} - I_o\left(\exp\left(\frac{V+IR_s\Gamma}{V_TN_{ss}}\right)+\exp\left(\frac{V+IR_s\Gamma}{(P-1)V_TN_{ss}}\right)-2\right)\right\} - \left(\frac{V+IR_s\Gamma}{R_p\Gamma}\right) \quad (6)$$

$$\Gamma = \frac{N_{ss}}{N_{pp}} \quad (7)$$

where N_{ss} and N_{pp} are the series and parallel PV modules in SP topology, respectively. More details of this model can be seen in [32].

It can be noted that in Eqs. (6) and (7), the series resistance in a solar cell/module is not apparent and if the solar cells that form the array are not identical, the factor $R_s\Gamma$ will not hold for an accurate mathematical model. A more detailed work in this direction is proposed in [33], where a method to optimize the SP configuration of solar array for various solar irradiation and climatic conditions was carried out. It provides a theoretical, step-by-step procedure to build up an array starting from the shape of an elemental cell to the largest assembly. The aim is to study the influence of various climates on the optimal PV cells interconnections. Furthermore, it highlights the dependence of the optimum cell interconnections on the cell quality and the types of module technologies. Whilst this approach results in a slightly more accurate model, it may complicate the main issue that is to be addressed by this paper, i.e. the solution to the partial shading on the module. Hence it is thought that the application a simpler model, as described in [32] would be more appropriate.

2.2. Partially shaded PV array

Fig. 2 shows a more realistic SP arrangement of a PV array: in this example, an array which consists of three modules per string is depicted. In addition, a blocking diode is connected in series to prevent reverse current from flowing back to the module. Furthermore, a bypass diode is connected in parallel to each module. Its function is to protect the module from becoming a hot-spot when PS occurs on that module.

For illustration, let's assume each PV module in Fig. 2 has a nominal rating of 20 W at STC. When the PV array receives a uniform irradiance of 1000 W/m^2, the parallel diodes are reversed biased. Consequently the PV current flows only due to the series PV modules, resulting in a P–V characteristics curve that exhibits a unique MPP. However, when PV array is subjected to PS, as shown in Fig. 2b, one of the modules receives a solar irradiance of 500 W/m^2, while others are at full irradiance of 1000 W/m^2. The difference in solar irradiance causes the shaded module to behave as a load instead of a generator, i.e. it tries to sink current generated by other (non-shaded) modules. With the presence of the bypass diode, that current is diverted away, preventing the shaded module from being damaged. However, the current diversion by the bypass diode transforms the P–V curves into more complicated shape – characterized by multiple peaks (several local and one global). As a result, two stairs of current are observed and the P–V curve is characterized by two peaks having a GP at 40 W. The blocking diode at the end of each string provides the protection against reverse current caused by the voltage mismatch between the parallel connected strings.

It can be noticed that by removing bypass diodes, the PV array exhibits only a single peak in P–V curve but with a much lower MPP, i.e. 30 W. It can therefore be noted that, in general, the bypass

diode improves the efficiency of PV array at the expense of more complicated *P–V* characteristics curves.

3. Particle swarm optimization

Particle swarm optimization (PSO) is a stochastic, population-based search method, modeled after the behavior of bird flocks [34]. A PSO algorithm maintains a swarm of individuals (called particles), where each particle represents a candidate solution. Particles follow a simple behavior: emulate the success of neighboring particles and its own achieved successes. The position of a particle is therefore influenced by the best particle in a neighborhood, P_{best}, as well as the best solution found by the particle, G_{best}. Particle position, x_i, is adjusted using the following equation:

$$x_i(k+1) = x_i(k) + v_i(k+1) \tag{8}$$

where the velocity component, v_i, represents the step size. The velocity is calculated by

$$v_i(k+1) = wv_i(k) + c_1r_1\{P_{best_i} - x_i(k)\} + c_2r_2\{G_{best} - x_i(k)\} \tag{9}$$

where w is the inertia weight, c_1 and c_2 are the acceleration coefficients, r_1, $r_2 \in U(0,1)$, $P_{best,i}$ is the personal best position of particle i, and G_{best} is the best position of the particles. The typical movement of particles in the optimization process is shown in Fig. 3.

4. Direct control structure

Fig. 4 shows the block diagram of a conventional MPPT scheme. Typically it consists of two independent control loops [35,36]. The first one is the voltage control loop that works by comparing the sensed PV voltage with a reference signal obtained from the MPPT block. The output of this loop is used as a reference for the second loop, i.e. the current control loop. The latter tries to bring the tracking error to zero at the MPP [35]. Since PI controllers are easy to design, inexpensive and low cost, they are widely used in these loops. However, due to the nonlinear characteristics of PV and unpredictable environmental conditions, PI controllers are not suited for standalone PV systems [25].

Alternatively, MPPT controller can be operated with the absence of control loops as mentioned above. This type is known as the direct MPPT control scheme; its general block diagram is shown in Fig. 4. Both the PI control loops are eliminated and duty cycle is computed directly in the algorithm. This scheme offers number of advantages: (1) it simplifies the tracking structure, (2) it reduces the computation time and (3) no tuning effort is needed for the PI gains. In short, it replaces sophisticated MPPT control with a more simplified structure while maintaining the optimal results.

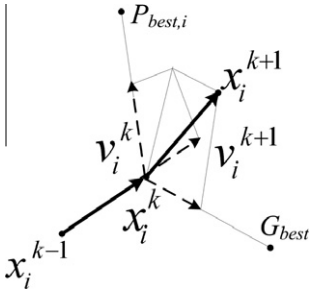

Fig. 3. Movement of particles in the optimization process.

5. Proposed direct control method using PSO to track the GP

In this work, a PSO algorithm is applied to track the MPP using the direct control technique. In order to start the optimization, a solution vector of duty cycles with Np particles needs to be defined as follows:

$$\begin{aligned} x_i^k &= d_g = [d_1, d_2, d_3, \ldots, d_j] \\ j &= 1, 2, 3, \ldots, Np \end{aligned} \tag{10}$$

The personal best position of particle P_{besti} is updated using Eq. (11) if the condition in Eq. (12) is satisfied, i.e.

$$P_{best,i} = x_i^k \tag{11}$$

$$f(x_i^k) > f(P_{best,i}) \tag{12}$$

where "f" is the objective function (operating power of PV array) for the tracking problem. Moreover, according to Eq. (9), the variable $P_{best,i}$ is used to memorize the best duty cycle (i.e. the duty cycle that yields maximum power) that the ith particle has found so far. The

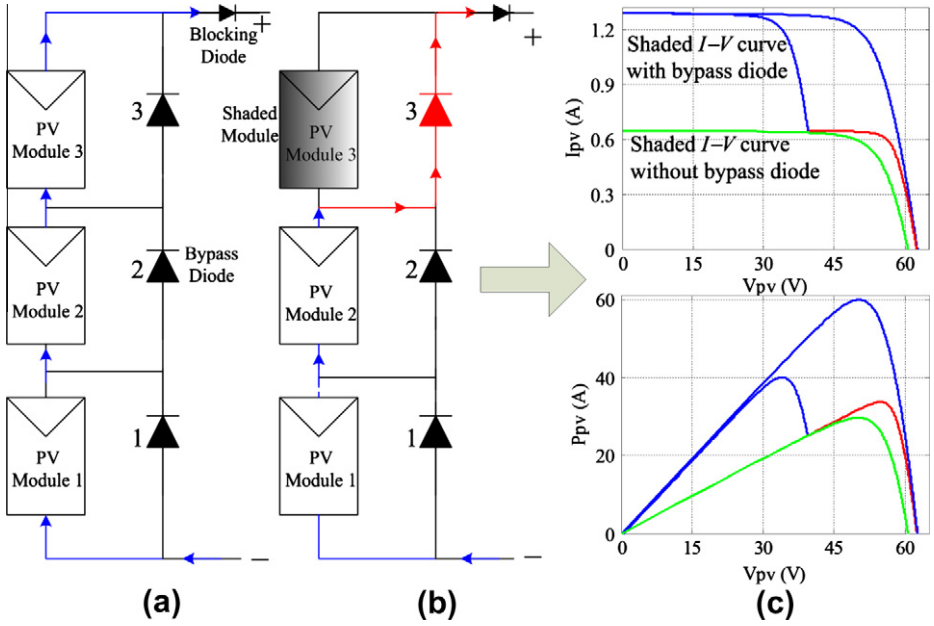

Fig. 2. operation of PV array (a) under uniform irradiation (b) under PS (c) the resulting *I–V* and *P–V* curve for (a) and (b).

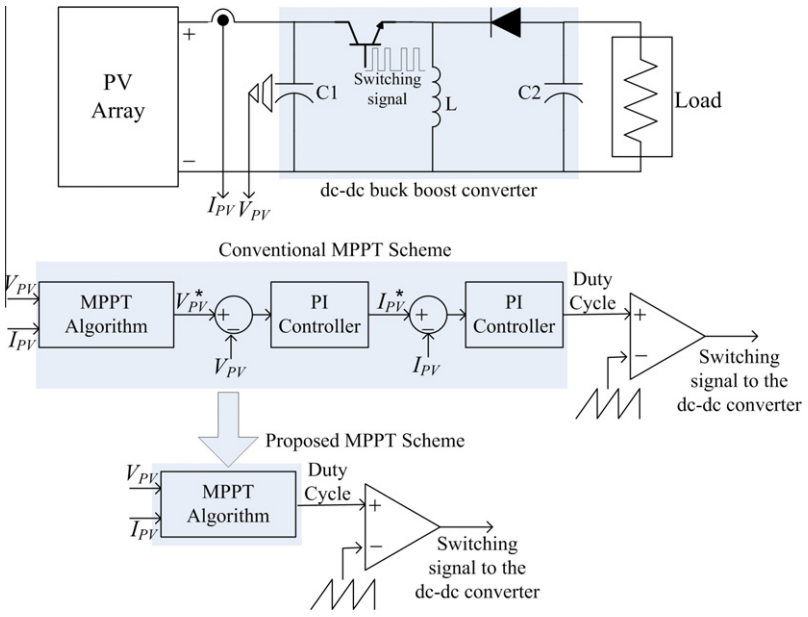

Fig. 4. Conventional and proposed direct control structure.

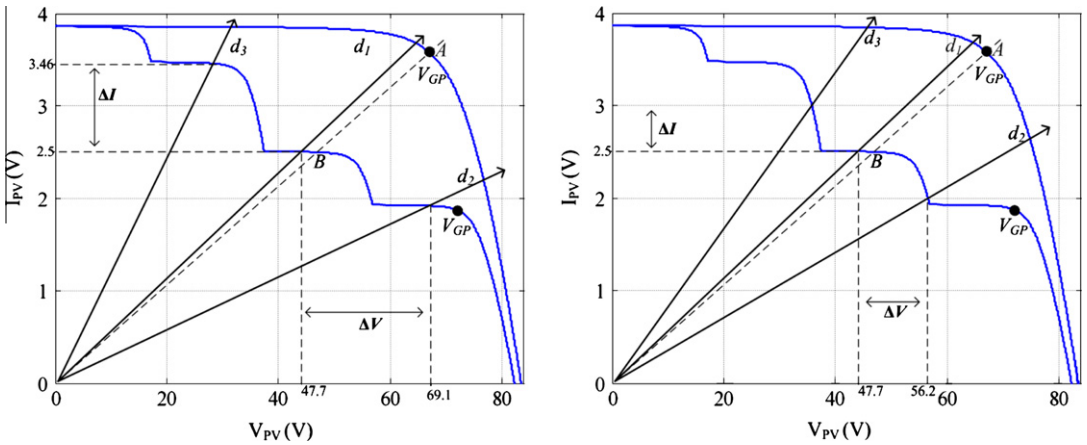

Fig. 5. Identification of PS condition (a) feasible range of duty cycles and (b) infeasible range of duty cycles.

variable G_{best} is used to memorize the best duty cycle achieved among all the particles.

When PV array is subjected to PS, its *I–V* curves exhibit multiple stairs while the *P–V* curves are characterized by multiple peaks [37,38]. Initially, it is assumed that the algorithm has successfully reached the MPP (point *A*) as shown in Fig. 5a. Once the PS occurs, the operating point moves from *A* to *B*. This results in reduction of the tracked power even though the duty cycle is not changed. To track a new MPP, the proposed algorithm switches to the "global" mode. In this mode, it transmits three duty cycles d_i (i = 1–3) to the power converter. To determine whether the system operates in uniform irradiance or PS, the following check is made:

$$\frac{I_{d3}-I_{d1}}{I_{d3}} \geqslant 0.1 \tag{13}$$

$$\frac{V_{d2}-V_{d1}}{V_{d2}} \geqslant 0.2 \tag{14}$$

If Eqs. (13) and (14) are satisfied, the PV array is known to operate in the PS condition. Note that the values obtained in Eqs. (13) and (14) are based on the observation that I_{mpp} and V_{mpp} are about 90% and 80% of I_{sc} and V_{oc} of a solitary *I–V* curve, respectively [24].

Once the occurrence of PS is confirmed by Eqs. (13) and (14), the proposed method activates the PSO algorithm. Using the information of the previous three duty cycles, it begins the searching procedure using Eqs. (9) and (10). When the change in velocity of the particles, Δv, reaches a predefined sufficiently small value, the search is terminated; it is assumed that the MPP has been reached. Then the algorithm switches to the "local" mode, which is the P&O method. A small perturbation step of 0.005 is employed in this mode. The reason for the switching from global to local mode is due to the better efficiency of the latter with respect to small changes in the irradiance or temperature.

It must be noted that if the initial (three) duty cycles could not cover of *I–V* curve ranging from V_{oc} to I_{sc}), the obtained information will not be feasible and PSO will not be activated. This observation is evident in Fig. 5b. The obtained information from applied duty cycles only satisfies Eq. (13). Consequently the algorithm will not go into PSO (global mode); instead it activates the P&O (local mode). As a result, it tracks the local MPP instead of global. This constraint can be solved using the idea of reflective impedance [24]. Using this concept, a feasible range of duty cycle for the buck-boost converter topology can be calculated using:

$$d_{\min} = \frac{\sqrt{\eta_{bb}R_{L\min}}}{\sqrt{R_{PV\max}} + \sqrt{\eta_{bb}R_{L\min}}} \tag{15}$$

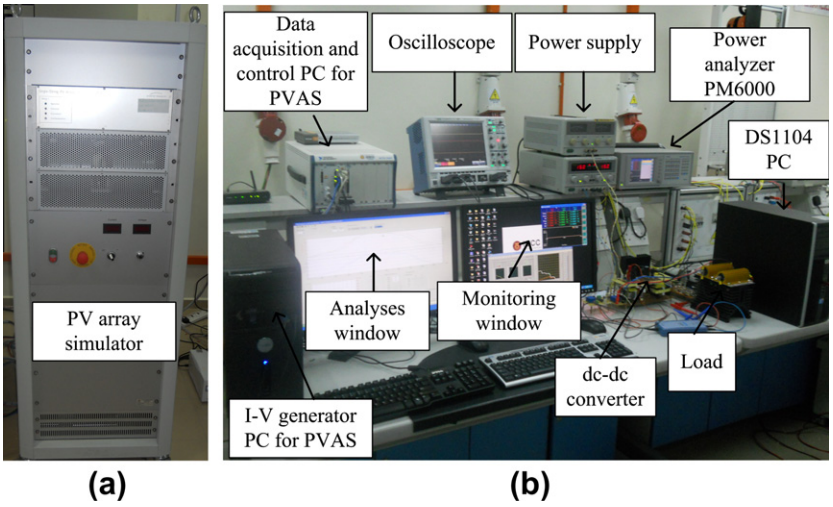

Fig. 6. (a) PVAS unit and (b) experimental setup of MPPT system.

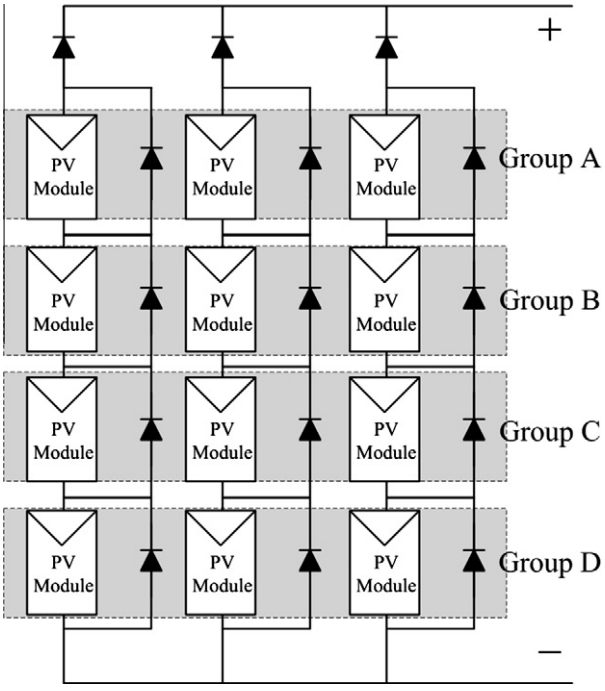

Fig. 7. PV array used in the experimental setup.

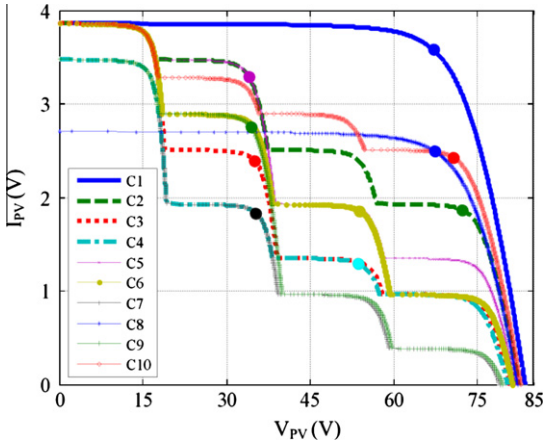

Fig. 8. Ten (10) different sets of *I–V* curve used in the experiment.

$$d_{\max} = \frac{\sqrt{\eta_{bb} R_{L\max}}}{\sqrt{R_{PV\min}} + \sqrt{\eta_{bb} R_{L\max}}} \tag{16}$$

where η_{bb} is the converter efficiency, $R_{L\min}$ and $R_{L\max}$ are minimum and maximum values of the connected load at the output, respectively. Variables $R_{PV\min}$ and $R_{PV\max}$ are the reflective impedances of a PV array.

The PSO parameters used in this work are as follows: $Np = 3$, $c_1 = 1.2$, $c_2 = 1.6$ and $w = 0.4$. These values are determined by trial and error method using simulations [28]. The pseudo code of the PSO is shown here. The operation of the algorithm in local mode (P&O) is omitted as the method is well explained elsewhere [11].

Step 1
Setting values of the control parameters of PSO:
Population size *NP*, inertia *w*, learning factors c_1 and c_2
Step 2: Initialization
Set the generation number $k = 0$
Initialize a population of *NP* individuals
Initialize velocities, v, of the particles:
Step 3
WHILE the stopping criterion is not satisfied
DO
FOR $i = 1$ to *NP*
Step 3: Calculate P_{best} and G_{best}
Evaluate the fitness of particles
IF $J(d_i^{k+1}) > J(d_i^k) THEN\ P_{best,i}^k = d_i^{k+1}$
ELSE $P_{best,i}^k = d_i^k$
ENDIF
$G_{best}^k = \max(P_{best,i}^k)$
Step 4: Update position and velocity
Calculate the velocities and positions of particles in the following way:
$v_i^{k+1} = w^* d_i^k + c_1^*(P_{best,i}^k d_i^k) + c_2^*(G_{best}^k d_i^k)$
$d_i^{k+1} = d_i^k + v_i^{k+1}$
END FOR
Step 5: Increase the generation count
$k = k + 1$
END WHILE

Table 1
Tracking results for the proposed and conventional direct control method.

Curve	Shading pattern (1 = 1000 W/m^2)				PVAS output			Proposed method			Work [11]			Efficiency (ηMPP)	
	A	B	C	D	V_{mp}	I_{mp}	P_{mp}	V_{mp}	I_{mp}	P_{mp}	V_{mp}	I_{mp}	P_{mp}	Proposed	Work [11]
1	1	1	1	1	67.1	3.58	240	67	3.58	239.9	67.7	3.55	239.6	99.94	99.84
2	1	0.9	0.65	0.5	72.2	1.87	135	70.6	1.89	133.1	53.3	2.42	128.9	98.59	95.54
3	1	0.65	0.35	0.25	35.1	2.39	84	35.0	2.39	83.65	34.9	2.40	83.76	99.58	99.71
4	0.9	0.5	0.35	0.25	53.3	1.30	69	53.7	1.29	68.74	35.0	1.85	64.75	99.62	93.84
5	0.9	0.5	0.35	1	33.7	3.321	112	34.1	3.28	111.8	34.5	3.22	111.1	99.86	99.18
6	1	0.75	0.5	0.25	53.9	1.86	100	53.4	1.87	99.67	34.9	2.72	94.93	99.67	94.92
7	0.9	0.15	0.25	0.1	35.2	1.84	65	35.1	1.84	64.58	35.5	1.80	63.90	99.36	98.31
8	0.7	0.7	0.7	0.7	67.0	2.50	168	67.1	2.50	167.7	65.4	2.55	166.1	99.85	98.88
9	0.25	0.9	0.75	0.1	34.3	2.76	95	34.5	2.74	94.53	34.2	2.75	94.05	99.50	99.00
10	1	0.85	0.75	0.65	70.4	2.44	172	68.5	2.48	169.9	52.3	2.78	144.9	98.77	84.22

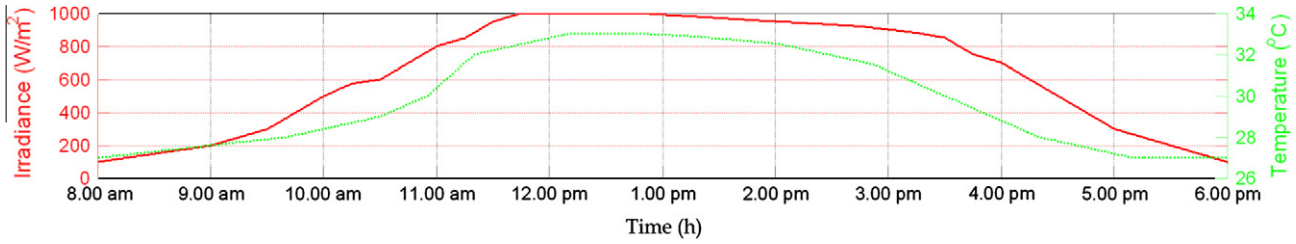

Fig. 9. Ten hour Malaysian daily profile [35,36].

6. Experimental setup

In this work, the PV array is emulated using the *PV Array Simulator*, PVAS [39], as shown in Fig. 6a. The PVAS consists of a linear power supply for the power stage and a current controller to generate the *I–V* curves. The latter is built using the voltage-controlled current-source concept. The *I–V* curves generation unit consists of an integrated RAM, which holds the template for the array characteristics; they are continuously updated with the new *I–V* data via a PC. A special firmware allows for a smooth and continuous transition between the *I–V* curves stored in each RAM. The PVAS provides real time simulation capabilities of any time series of irradiance, temperature, fill factor or any arbitrary *I–V* curves measured at real testing conditions. Unlike the conventional PV array simulators with diode strings, the usage of digital control with precisely defined characteristics allows the exact knowledge of MPP for every time step. Hence, the high precision dynamic MPPT measurements are possible. Furthermore, due to the linear power stage, the problem of switching frequency induced by the simulator does not arise.

The overall experimental setup of the MPPT system implemented in this work is shown in Fig. 6b. A buck-boost converter with the following specifications is used: $C_1 = 470\ \mu$F, $C_2 = 220\ \mu$F, $L = 1$ mH. The converter is switched at 50 kHz. To ensure the system attains the steady state before another MPPT cycle is initiated, the sampling interval is chosen as 0.05 s.

The PV array configuration that is used to emulate the actual *I–V* curves is shown in Fig. 7. It comprises of three strings, each having four series-connected modules. Each module is rated at STC as follows: $P_{MAX} = 20$ W, $I_{MPP} = 1.21$ A, $V_{MPP} = 16.8$ V, $I_{SC} = 1.29$ A, and $V_{OC} = 21$ V. For simplicity, module based shading is considered. The array is characterized in four groups namely, *A*, *B*, *C*, and *D*. Each group can be configured for a different shading and temperature condition.

7. Results and discussion

The tracking performance of the proposed method is tested using ten different *I–V* curves, as shown in Fig. 8. These curves are generated using [40] by imposing various shading patterns on the PV array model (Fig. 7). The first curve (C1) is the normal condition with uniform irradiation. The subsequent curves (*C*2–*C*9) are partial shading curves, generated at a transition rate of 10 s. Once the curves are prepared, they are stored in the PVAS RAM. Whenever required, a particular curve will be powered (using the PVAS power stage) to generate the real *I–V* output.

To evaluate the effectiveness of the proposed method, its performance is compared with the conventional direct control approach described in [11].

Table 1 summarizes the tracked voltage, current, and power for the proposed approach and the method described in [11]. It can be observed that for all the ten *I–V* curves under examination, the GP exists in a certain region i.e. 30–70 V. This also confirms the validity of Eqs. (15) and (16) for calculating $d_{\min}$ and $d_{\max}$. In general, the proposed method accurately tracks the global MPP for all given shading conditions. It yields more than 99.5% efficiency except for the curves C2 and C10. For these two cases, the MPP is in the vicinity of V_{OC}. Once the converter operates at this region, a considerable oscillation in array power is experienced. This is due to the oscillation in the array voltage. Such observation is also in close agreement with the work in [23].

On the other hand, the tracking performance using the method described in [11] can be considered as unsatisfactory. In most cases, the algorithm is trapped at the local maxima. This is more crucial for the curve C10 – only 84.2% of the output power could be extracted from the PV array. It can be seen that for certain shading patterns, the algorithm tracks the GP correctly. This is because when the operating point shifts from the previous *I–V* curve to the current one, the new operating point falls in the vicinity of the GP region. Accordingly, due to its hill climbing nature, the method described in [11] eventually tracks the correct GP.

To further validate the effectiveness of the proposed method in real environmental condition, an experiment is conducted using the actual weather profile of Malaysia (a tropical country, near the Equator) obtained from the work carried out in [41]. The profile simulates the hourly sunlight of the Malaysian sky using daylight modeling. The model is based on empirical and measured solar irradiation and cloud cover data. To produce the exterior irradiance data, measurements are made at two locations in the country.

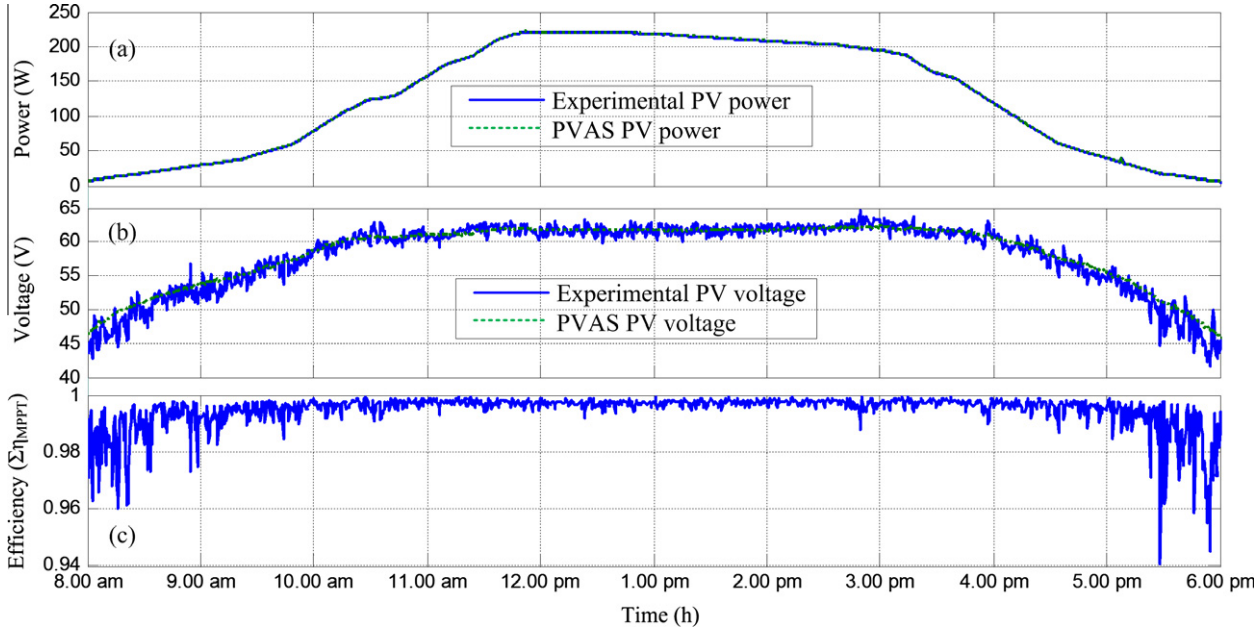

Fig. 10. Experimental results for the 10 h (8.00 am–6.00 pm) Malaysian profile (a) MPPT power (b) MPPT voltage and (c) MPPT efficiency.

Fig. 9 shows the resulting irradiance and temperature profile for a typical daylight in Malaysia, i.e. 8.00 am–6.00 pm (10 h) obtained from [41,42]. This 10 h irradiance and temperature profile (Fig. 9) is loaded into the PVAS. Then the power supply of the PVAS generates the power output and feed to the buck-boost converter that employs the propose MPPT control.

Fig. 10a–c shows the experimental results for the array power, voltage and efficiency for the proposed method using the environmental profile shown in Fig. 9. The data is recorded with a sampling rate of 1 s. It can be clearly seen that for the whole profile of 10 h, MPP tracking performed by the proposed method is extremely accurate – as evidenced by the exact superimposing of the experimental and PVAS output power. It can be seen that proposed method yields an average efficiency of 99.5%. However, it can be noticed that efficiency at very low power (low insolation) is relatively less. This is due to the fact that at low insolation, very low current is drawn from the PV array; consequently, even a small perturbation step (0.005) results a significant variation in the current, which in turn causing severe oscillations in the PV voltage at MPP. This observation can be clearly related to Fig. 10b.

8. Conclusion

In this work, an improved MPPT technique based on particle swarm optimization (PSO) algorithm is proposed. The method directly computes the duty cycle and eliminates the need for PI control loops. It overcomes the weaknesses of conventional direct control method particularly in partial shading conditions. Experimental results have shown that the proposed method outperforms the conventional method in terms of tracking performance under ten different irradiance conditions, including various patterns for partial shading. In average, the proposed method yields 99.5% efficiency. Furthermore, the algorithm is tested using a 10 h irradiance and temperature profile of Malaysia. Using a solar array simulator, the average MPPT efficiency of 99.5% is achieved.

Acknowledgments

This research work was supported by the Universiti Teknologi Malaysia and funded by Ministry of Higher Education Malaysia under Grant 68704.

References

[1] Kuznetsov IA, Greenfield MJ, Mehta YU, Merchan-Merchan W, Salkar G, Saveliev AV. Increasing the solar cell power output by coating with transition metal-oxide nanorods. Appl Energy 2011;88:4218–21.
[2] Li M, Ji X, Li G, Wei S, Li Y, Shi F. Performance study of solar cell arrays based on a trough concentrating photovoltaic/thermal system. Appl Energy 2011;88:3218–27.
[3] Han X, Wang Y, Zhu L. Electrical and thermal performance of silicon concentrator solar cells immersed in dielectric liquids. Appl Energy 2011;88:4481–9.
[4] Zhang W, Zhu R, Liu B, Ramakrishna S. High-performance hybrid solar cells employing metal-free organic dye modified TiO_2 as photoelectrode. Appl Energy 2012;90:305–8.
[5] Li M, Liu Y, Wang H, Shen H. Synthesis of TiO_2 submicro-rings and their application in dye-sensitized solar cell. Appl Energy 2011;88:825–30.
[6] Qiao L, Wang D, Zuo L, Ye Y, Qian J, Chen H, et al. Localized surface plasmon resonance enhanced organic solar cell with gold nanospheres. Appl Energy 2011;88:848–52.
[7] Xu HB, Hong RJ, Ai B, Zhuang L, Shen H. Application of phosphorus diffusion gettering process on upgraded metallurgical grade Si wafers and solar cells. Appl Energy 2010;87:3425–30.
[8] Chou CS, Guo MG, Liu KH, Chen YS. Preparation of TiO_2 particles and their applications in the light scattering layer of a dye-sensitized solar cell. Appl Energy 2012;92:223–4.
[9] Ishaque K, Salam Z, Syafaruddin. A comprehensive MATLAB Simulink PV system simulator with partial shading capability based on two-diode model. Solar Energy 2011;85:2217–27.
[10] Bruendlinger R, Bletterie B, Milde M, Oldenkamp H. Maximum power point tracking performance under partially shaded PV array conditions. In: Proc. 21st EUPVSEC, Germany; 2006. p. 2157–60.
[11] Fermia N, Granozio D, Petrone G, Vitelli M. Predictive and adaptive MPPT perturb and observe method. Aerosp Electron Syst IEEE Trans 2007;43:934–50.
[12] Femia N, Petrone G, Spagnuolo G, Vitelli M. Optimization of perturb and observe maximum power point tracking method. Power Electron IEEE Trans 2005;20:963–73.
[13] Lin C-H, Huang C-H, Du Y-C, Chen J-L. Maximum photovoltaic power tracking for the PV array using the fractional-order incremental conductance method. Appl Energy 2011;88:4840–7.
[14] Safari A, Mekhilef S. Simulation and hardware implementation of incremental conductance MPPT with direct control method using Cuk converter. Indust Electron IEEE Trans 2011;58:1154–61.
[15] Esram T, Kimball JW, Krein PT, Chapman PL, Midya P. Dynamic maximum power point tracking of photovoltaic arrays using ripple correlation control. Power Electron IEEE Trans 2006;21:1282–91.
[16] Noguchi T, Togashi S, Nakamoto R. Short-current pulse-based maximum-power-point tracking method for multiple photovoltaic-and-converter module system. Indust Electron IEEE Trans 2002;49:217–23.
[17] Dorofte C, Borup U, Blaabjerg F. A combined two-method MPPT control scheme for grid-connected photovoltaic systems. In: Power electronics and applications, 2005 European conference on; 2005. p. P.1–P.10.

[18] Kyoungsoo R, Rahman S. Two-loop controller for maximizing performance of a grid-connected photovoltaic-fuel cell hybrid power plant. Energy Convers IEEE Trans 1998;13:276–81.
[19] Rai AK, Kaushika ND, Singh B, Agarwal N. Simulation model of ANN based maximum power point tracking controller for solar PV system. Sol Energy Mater Sol Cell 2011;95:773–8.
[20] Kobayashi K, Takano I, Sawada Y. A study of a two stage maximum power point tracking control of a photovoltaic system under partially shaded insolation conditions. Sol Energy Mater Sol Cell 2006;90:2975–88.
[21] Karatepe E, Hiyama T, Boztepe M, Çolak M. Voltage based power compensation system for photovoltaic generation system under partially shaded insolation conditions. Energy Convers Manage 2008;49:2307–16.
[22] Miyatake M, Inada T, Hiratsuka I, Hongyan Z, Otsuka H, Nakano M. Control characteristics of a fibonacci-search-based maximum power point tracker when a photovoltaic array is partially shaded. In: 4th International on power electronics and motion control conference, vol. 2; 2004. p. 816–21.
[23] Patel H, Agarwal V. Maximum power point tracking scheme for PV systems operating under partially shaded conditions. Indust Electron IEEE Trans 2008;55:1689–98.
[24] Tat Luat N, Kay-Soon L. A global maximum power point tracking scheme employing DIRECT search algorithm for photovoltaic systems. Indust Electron IEEE Trans 2010;57:3456–67.
[25] Salem F, Adel Moteleb Mohamed S, Dorrah HT. An enhanced fuzzy-PI controller applied to the MPPT problem. J Sci Eng 2005;8:147–53.
[26] Ishaque K, Salam Z. An improved modeling method to determine the model parameters of photovoltaic (PV) modules using differential evolution (DE). Solar Energy 2011;85:2349–59.
[27] Ishaque K, Salam Z, Taheri H, Shamsudin A. A critical evaluation of EA computational methods for photovoltaic cell parameter extraction based on two diode model. Solar Energy 2011;85:1768–79.
[28] Miyatake M, Veerachary M, Toriumi F, Fujii N, Ko H. Maximum power point tracking of multiple photovoltaic arrays: a particle swarm optimization approach. Aerosp Electron Syst IEEE Trans 2011;47:367–80.
[29] Roy Chowdhury S, Saha H. Maximum power point tracking of partially shaded solar photovoltaic arrays. Sol Energy Mater Sol Cell 2010;94:1441–7.
[30] dSPACE GmbH. DS1104 RTLib reference. Paderborn (Germany): User's Guide; 2004.
[31] Chih-Tang S, Noyce RN, Shockley W. Carrier generation and recombination in P–N junctions and P–N junction characteristics. Proc IRE 1957;45:1228–43.
[32] Ishaque K, Salam Z, Taheri H. Simple, fast and accurate two-diode model for photovoltaic modules. Sol Energy Mater Sol Cell 2011;95:586–94.
[33] Badescu V. Simple optimization procedure for silicon-based solar cell interconnection in a series-parallel PV module. Energy Convers Manage 2006;47:1146–58.
[34] Eberhart R, Kennedy J. A new optimizer using particle swarm theory. In: Micromachine and human science, 1995. MHS '95' Proceedings of the sixth international symposium on; 1995. p. 39–43.
[35] Esram T, Chapman PL. Comparison of photovoltaic array maximum power point tracking techniques. Energy Convers IEEE Trans 2007;22:439–49.
[36] Young-Hyok J, Doo-Yong J, Jun-Gu K, Jae-Hyung K, Tae-Won L, Chung-Yuen W. A real maximum power point tracking method for mismatching compensation in PV array under partially shaded conditions. Power Electron IEEE Trans 2011;26:1001–9.
[37] Ishaque K, Salam Z, Taheri H, Syafaruddin. Modeling and simulation of photovoltaic (PV) system during partial shading based on a two-diode model. Simul Mod Pract Theor 2011;19:1613–26.
[38] Patel H, Agarwal V. MATLAB-based modeling to study the effects of partial shading on PV array characteristics. Energy Convers IEEE Trans 2008;23:302–10.
[39] User's Manual. Programmable photovoltaic array simulator PVAS1. Arsenal Research, Austrian Institute of Technology (AIT); 2007.
[40] Ishaque K, Salam Z, Taheri H. Accurate MATLAB simulink PV system simulator based on a two-diode model. J Power Electron 2011;11:9.
[41] Zain-Ahmed A, Sopian K, Zainol Abidin Z, Othman MYH. The availability of daylight from tropical skies – a case study of Malaysia. Renew Energy 2002;25:21–30.
[42] Azli NA, Salam Z, Jusoh A, Facta M, Lim BC, Hossain S. MPPT performance of a grid-connected PV inverter under Malaysian conditions. In: Power and energy conference, 2008. PECon 2008. IEEE 2nd international; 2008. p. 457–9.